

# BEAM-BASED RECONSTRUCTION OF THE SHIELDED QUENCH-HEATER FIELDS FOR THE LHC MAIN DIPOLES\*

L. Richtmann<sup>†</sup>, L. Bortot, E. Ravaoli, C. Wiesner, D. Wollmann  
CERN, CH-1211 Geneva, Switzerland

## Abstract

Small orbit oscillations of the circulating particle beams have been observed immediately following quenches in the LHC's superconducting main dipole magnets. Magnetic fields generated during the discharge into the quench heaters were identified as the cause. Since the resulting, shielded field inside the beam screen cannot be measured in-situ, the time evolution of the field has to be reconstructed from the measured beam excursions.

In this paper, the field-reconstruction method using rotation in normalized phase space and the optimized fitting algorithm are described. The resulting rise times and magnetic field levels are presented for quench events that occurred during regular operation as well as for dedicated beam experiments. Finally, different approaches to model the shielding behavior of the beam screen are discussed.

## INTRODUCTION AND MOTIVATION

The Large Hadron Collider (LHC) at CERN uses superconducting dipole magnets to guide the particles around their circular trajectory. The energy stored in each of the 8 main dipole circuits, comprising 154 magnets each, is around 1 GJ. Therefore, a sophisticated Quench Protection System (QPS) is installed to avoid damage in case of a resistive transition (quench) in one of the magnet coils [1–3].

An essential part of the QPS are the so-called quench heaters [4] that uniformly heat up the entire superconducting coil after the detection of a quench to avoid a local temperature hot spot. In case of a quench, a nominal current of 75 A [5, p. 174] is discharged through the quench heater strips that are attached to the outer part of each LHC dipole coil. To protect the superconducting coils from beam-induced heating and secondary particles, the beams travel inside a stainless-steel beam screen, which has a co-laminated copper layer with a nominal thickness of 75  $\mu\text{m}$  [5, 6].

During Run 2 of the LHC (2015-2018), it was recognized that the magnetic field generated during the discharge of the quench heaters can cause oscillations of the circulating beam [7]. Although this effect is not considered critical for the current LHC operation, the fast development of the orbit perturbation has triggered detailed studies to understand its criticality for High Luminosity (HL)-LHC operation [7, 8].

Since the resulting field inside the beam screen cannot be measured in-situ, a method was developed to reconstruct it based on the measured beam excursions [9], which is a crucial input for any shielding model.

\* This research was supported by the HL-LHC project.

<sup>†</sup> Lea.richtmann@aei.mpg.de

## RECONSTRUCTION OF THE QUENCH-HEATER FIELD

### BPM Measurements

In each of the two LHC rings, 516 Beam Position Monitors (BPM) are installed [5, ch. 13]. They measure the beam position averaged over all circulating bunches with a turn-by-turn resolution. Figure 1 shows the beam position measured by one BPM over 50 LHC turns after the firing of the quench heaters in one dipole magnet. The orbit deviation after the quench heater firing, taking effect at turn 14, can clearly be observed. Since the quench heaters produce a horizontal dipole field, the beam is displaced in the vertical plane [7, 8]. In contrast, a reduction of the main dipole field following the quench would displace the beam in the horizontal plane and would occur only on a time scale of tens of milliseconds.

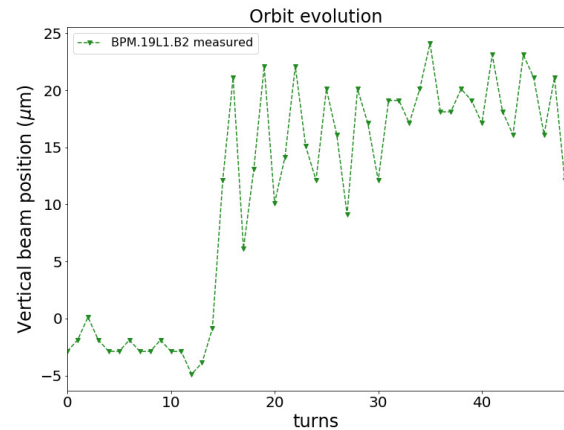


Figure 1: Example of the displacement of Beam 2 measured at one BPM after the firing of the quench heaters (timestamp: 2016-07-12 14:17:13, beam mode: collision, beam energy: 6.5 TeV, 1807 bunches per beam circulating). One LHC turn corresponds to a revolution time of 89  $\mu\text{s}$ .

From the measured beam positions, one can then calculate the change of momentum or angle for each turn, which allows to reconstruct the magnetic field causing this change by using the method described in the following section.

### Field-Reconstruction Method

For this method [9], it is assumed that the beam is kicked at one single location with a pure dipole field. However, no specific assumption on the time profile of the kick is made, such that this method can also be used for other cases.

In general, the envelope of a particle beam can be described by an ellipse in phase space [10], defined by the position  $y$  and the angle  $y'$ . By normalizing the position

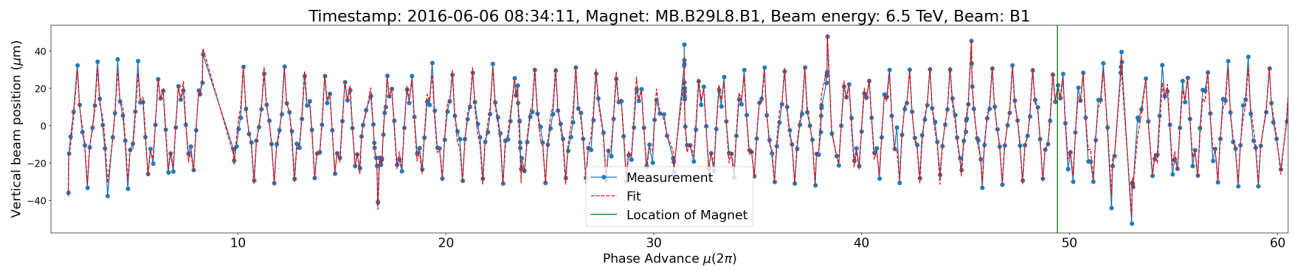


Figure 2: Comparison of the measured (blue) and fitted (red) beam positions around the complete LHC ring five turns after the firing of the quench heaters. The location of the magnet where the kick occurs is indicated with a green line.

and angle using the twiss parameters [9, p. 6], the ellipse becomes a circle, allowing to calculate the change of the beam coordinates at different locations in the ring by rotation in normalized phase space [10, p. 173].

If a magnetic field provides a kick to the beam at a location  $M$ , this causes a change in the momentum or angle. To determine the beam position and angle in the current turn  $n$ , one, thus, has to rotate the coordinates from the previous turn  $(n - 1)$  by the vertical tune  $Q_y$  and then add the kick angle that the beam receives in this turn  $\theta_{\text{kick}}^n$  (see Eq. 1).

$$\begin{pmatrix} y_M^n \\ y_M^n \end{pmatrix} = \begin{pmatrix} \cos(Q_y) & \sin(Q_y) \\ -\sin(Q_y) & \cos(Q_y) \end{pmatrix} \begin{pmatrix} y_M^{n-1} \\ y_M^{n-1} \end{pmatrix} + \begin{pmatrix} 0 \\ \theta_{\text{kick}}^n \end{pmatrix} \quad (1)$$

To determine the impact of this kick at any other element in the ring, one can rotate the coordinates  $(y_M^n, y_M^n)$  by the phase advance between the kick location  $M$  and the desired element. This means, if position and angle at  $M$  from the turn before, as well as the kick angle given in this turn and the phase advance to the desired element are known, one can obtain a function that calculates the position at any desired element, i.e. at the BPMs. This function can then serve as a fitting function.

The beam positions at the BPMs are known from measurements. The phase advance to the kick location and the  $\beta$  function at the BPMs are known from the LHC optics models [11], which are implemented in MAD-X [12]. They are validated with measurements with a remaining  $\beta$  beating below 2% root mean square (rms) [13]. What remains unknown are the beam position and angle at the magnet and the kick angle  $\theta_{\text{kick}}^n$ . These unknown values are, thus, fitted using the large number of available BPM measurements.

It was, however, observed that a fit leaving all these parameters free led to un-physically large values in position and angle at the magnet. Therefore, an optimised algorithm was developed where the initial values  $(y, y')$  at the magnet are fitted for a turn before the kick happens. Afterwards, these coordinates are calculated analytically via rotation by the tune, such that the kick angle remains the only variable to be fitted. This method significantly improved the quality and consistency of the beam-based reconstruction compared to the initial approach.

Figure 2 shows an example of the fitting result. The BPM measurements around the complete ring for one turn are

compared with the beam positions as predicted with the fit function, giving an rms deviation of 3  $\mu\text{m}$ .

After obtaining the kick angle, one can transform the coordinates back into un-normalised phase space and calculate the kick field with Eq. 2:

$$B_x^n = \frac{\theta_{\text{kick}}^n \cdot B\rho}{\sqrt{\beta_M} \cdot L_M}, \quad (2)$$

where  $B\rho$  is the beam rigidity,  $\beta_M$  is the  $\beta$ -function at the magnet, and  $L_M = 14.3$  m is the magnetic length [5, p. 164]. As final results, one obtains the time evolution of the field inside the beam screen with a resolution of one turn.

In addition, it was verified that there was no significant impact on the reconstructed field due to the missing synchronisation between the turn-by-turn logging of the BPM data and the firing of the quench heaters [9, p. 29].

## FIELD-RECONSTRUCTION RESULTS

Figure 3 shows the reconstructed fields for all known quench events that led to a beam excursion during Run 2 of the LHC at flat-top (triangular markers) and at injection energy (round markers) during proton operation. For easier comparison, the fields are scaled to the same nominal quench heater current of 75 A, and the fields for Beam 2, which have negative sign, are multiplied by  $(-1)$ .

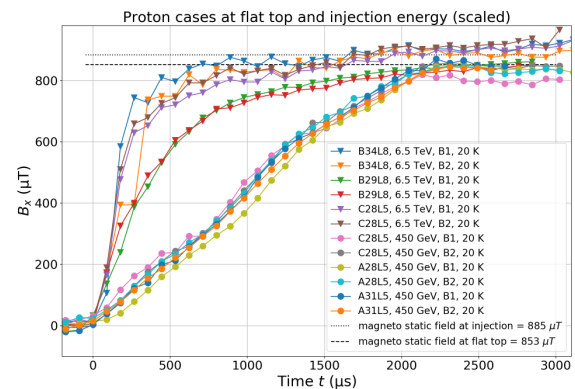


Figure 3: The reconstructed fields for all proton events at flat-top (6.5 TeV) and injection energy (450 GeV). The legend indicates the name of the dipole magnet where the quench heaters fired, the beam energy, the beam (B1/B2) and the temperature of the beam screen.

All reconstructed fields reach within a spread of 10 % the same level. In addition, the field levels agree very well with the expected magneto-static quench heater field (885  $\mu\text{T}$  at injection, 853  $\mu\text{T}$  at flat-top energy), which was independently calculated using the finite-element-method (FEM) code COMSOL [14] including the contribution of the surrounding iron. To quantify the rise times, the reconstructed field  $B(t)$  was fitted with a double exponential function:

$$B(t) = a(1 - \exp(-t/\tau_1))(\exp(-t/\tau_2)) \quad (3)$$

with the time constants  $\tau_1$  for the first initial rise,  $\tau_2$  for the second rise and the amplitude factor  $a$ . This ansatz was chosen because the current in the quench heater circuits is described by the same type of function.

For the LHC dipole magnet C28L5, beam-based measurements are available for the following four cases: Case a) quenches during dedicated beam experiments performed at injection energy with the nominal beam screen temperature of 20 K [15], Case b) quench during regular operation at 6.5 TeV with the nominal beam screen temperature, Cases c) and d) quenches during dedicated beam experiments performed with an increased beam screen temperature of 70 K at 3.5 TeV and 6.5 TeV, respectively [16]. Note that the fields for Cases c and d were reconstructed based on the beam positions measured with the ADTObsBox, which allows for a bunch-by-bunch resolution [16]. The reconstructed rise times are shown in Table 1. The errors were estimated taking into account the time resolution of the BPMs as well as one standard deviation for the error of the fit algorithm [9, p. 41]

Table 1: Reconstructed rise times  $\tau_1$ , rise times  $\tau_{\text{sim}}$  simulated with Model III (see below) and nominal copper resistivities  $\rho(B, T)$  [17] of the beam screen for four quench events available for dipole C28L5 for Beam 1.

Case	$\rho(B, T)$ ( $10^{-10} \Omega \text{m}$ )	$\tau_1$ ( $\mu\text{s}$ )	$\tau_{\text{sim}}$ ( $\mu\text{s}$ )
a) 450 GeV, 20 K	2.50	1900 $\pm$ 200	2790
b) 6.5 TeV, 20 K	5.28	250 $\pm$ 90	1290
c) 3.5 TeV, 70 K	18.20	170 $\pm$ 30	380
d) 6.5 TeV, 70 K	19.33	140 $\pm$ 30	360

As expected, the reconstructed field rise inside the beam screen is much slower than the rise of the external quench heater field, which has a time constant of  $\tau_1 = 7.5 \mu\text{s}$ . It can be observed that the field rises faster at flat-top than at injection energy. This is to be expected because the shielding efficiency of the beam screen depends on its copper resistivity, which changes with the main dipole field (or beam energy) due to magnetoresistivity and with temperature.

## SHIELDING MODELS AND OUTLOOK

It was noticed that the fields reconstructed from the beam position measurements rise faster than expected from FEM simulations. Therefore, several additional models were lever-

aged to simulate and cross-check the shielding behaviour of the beam screen [9]:

- Model I: A model that calculates analytically the eddy currents for a simplified geometry and takes explicitly the skin effect into account [18].
- Model II: A model of the shielding as a magnetic diffusion process, allowing for an analytical calculation of its time constant.
- Model III: The shielding was calculated with the script used for Model I [18], but using input fields that oscillate at fixed frequencies. From the field attenuation, the transfer function was derived, allowing for a calculation of the time constant by determining the cutoff frequency of the low-pass filter [9, p. 77].

All models predict an increased rise time of the field inside the beam screen when compared to the external quench heater field. It was found that all three models give consistent predictions of the rise time [9]. However, even though the simulated rise times agree better with the measurements than in previous studies, the models still predict more shielding than observed experimentally. Table 1 compares the reconstructed rise times with the ones simulated with Model III. Compared to the reconstruction, the simulated time constants are 1.5 times longer for Case a, about 2 times longer for Cases c and d, but 5 times longer for the quench events during regular LHC operation (Case b) [9].

As the models yield consistent results among them and as there is no indication that the input parameters are more than 20 % off, it was concluded that the models are incomplete. In particular, all models used so far were 2D models that do not take into account how the eddy current loops close. 3D effects could thus be responsible for the observed discrepancy and should be included in the future.

## CONCLUSION

A fully developed method to reconstruct the magnetic fields that are responsible for beam excursions observed after the firing of the quench heaters at the LHC main dipole magnets is presented. The method is based on the measured BPM data and uses rotation in normalized phase space. Since no assumption about the time evolution of the kick is made, this method can be applied generally.

The fields were reconstructed for different quench events. The resulting field levels agree within 10 % between the events and with magnetostatic calculations. Simulations using different 2D shielding models predict rise times that are a factor 1.5 to 5 longer than the ones from the beam-based reconstruction but are consistent among the models.

## ACKNOWLEDGMENTS

The authors would like to thank M. Morrone for important input and discussions about the beam screen, J. Wenninger for support with the BPM data and M. Maciejewski for help with querying data from the Post Mortem System.

## REFERENCES

- [1] M. Wilson, *Superconducting Magnets*. Clarendon Press, 1987.
- [2] R. Schmidt *et al.*, “Protection of the CERN Large Hadron Collider”, *New Journal of Physics*, vol. 8, no. 11, p. 290, Nov. 2006. doi : 10.1088/1367-2630/8/11/290
- [3] R. Denz, K. Dahlerup-Petersen, and K. H. Mess, “Electronic Systems for the Protection of Superconducting Devices in the LHC”, in *Proc. EPAC’08*, Genoa, Italy, Jun. 2008, pp. 2422–2424.
- [4] F. Sonnemann and F. Rodriguez-Mateos, “Quench Heater Studies for the LHC Magnets”, in *Proc. PAC’01*, Chicago, IL, USA, Jun. 2001.
- [5] O. Brüning (ed.) *et al.*, “LHC Design Report, Vol. I: The LHC Main Ring”, CERN, Geneva, Switzerland, Rep. CERN-2004-003, 2004.
- [6] M. Morrone, M. Martino, R. De Maria, M. Fitterer, and C. Garion, “Magnetic Frequency Response of High-Luminosity Large Hadron Collider Beam Screens”, *Phys. Rev. Accel. Beams*, vol. 22, p. 013501, Jan. 2019. doi : 10.1103/PhysRevAccelBeams.22.013501
- [7] M. Valette *et al.*, “Impact of Superconducting Magnet Protection Equipment on the Circulating Beam in HL-LHC”, in *Proc. IPAC’18*, Vancouver, Canada, Apr.-May 2018, pp. 3115–3118. doi : 10.18429/JACoW-IPAC2018-THPAF062
- [8] B. Lindstrom *et al.*, “Fast failures in the LHC and the future high luminosity LHC”, *Phys. Rev. Accel. Beams*, vol. 23, p. 081001, Aug. 2020. doi : 10.1103/PhysRevAccelBeams.23.081001
- [9] L. Richtmann, “Effect of Quench Heater Discharges on the Circulating Beam in the Large Hadron Collider”, M.S. thesis, Sep. 2021.
- [10] H. Wiedemann, *Particle Accelerator Physics*. Heidelberg New York Dordrecht London: Springer International Publishing, 2015.
- [11] *LHC Optics Web: LHC Run II pp physics optics*, [http://abpdata.web.cern.ch/abpdata/lhc\\_optics\\_web/www/opt2018/](http://abpdata.web.cern.ch/abpdata/lhc_optics_web/www/opt2018/).
- [12] MAD-X, <http://madx.web.cern.ch/madx/>.
- [13] T. Persson *et al.*, “LHC optics commissioning: A journey towards 1% optics control”, *Phys. Rev. Accel. Beams*, vol. 20, p. 061002, Jun. 2017. doi : 10.1103/PhysRevAccelBeams.20.061002
- [14] *Comsol multiphysics®*, [www.comsol.com](http://www.comsol.com). COMSOL AB, Stockholm, Sweden.
- [15] M. Valette *et al.*, “MD 1826: Measurement of Quench Heater vertical kick”, CERN, Geneva, Switzerland, Rep. CERN-ACC-2018-0007, Feb. 2018.
- [16] C. Wiesner *et al.*, “LHC MD 3205: Beam Screen Shielding from QH Discharge at 70 K”, CERN, Geneva, Switzerland, Rep. CERN-ACC-NOTE-2020-0003, Jan. 2020.
- [17] N. Simon, E. Drexler, and R. Reed, “Properties of copper and copper alloys at cryogenic temperatures. Final report”, Boulder, CO (United States). Materials Reliability Div., Tech. Rep. MONO-177, 1992.
- [18] E. Ravaioli and C. Wiesner, “Calculation of magnetic transients due to quench-heater discharges and eddy currents in cylindrical beam screens”, CERN, Geneva, Switzerland, MPE Technical Note 2021-01, EDMS Nr. 2470088, Jan. 2021, <https://edms.cern.ch/document/2470088>.